Clinical Neuroimaging at 7T Compared to Lower Field: a Photo Essay

Stephen E. Jones, Ph.D., M.D.[1]; Emmanuel Obusez, M.D.[1]; Sehong Oh, Ph.D.[1]; Irene Wang, Ph.D.[2]; Mark Lowe, Ph.D.[1]

Imaging Institute (1), Epilepsy Center (2), Cleveland Clinic, Cleveland, OH, USA

Introduction

The recent introduction of a clinical 7T human MRI scanner continues the progress of increasing field strength, ever since the invention of MRI. While research is understandably emphasized as the initial application when a new higher field MRI system is commercially introduced, inevitably clinical applications become the majority appliation. Similarly, such 7T scanners as are currently available are used mainly for research. However, with anticipated FDA approval in the next few years, 7T MRI will become clinically available. While the research utility of 7T is already clear, especially in functional brain imaging using BOLD fMRI [1-4], the clinical utility is uncertain at this time.

The main advantage of using higher magentic field is an increased signal from precessing magnetic moments, which scales as the field strength increases [5]. The increased signal improves images in several ways: Images with the same voxel size but higher signal-to-noise ratio (SNR), images with smaller voxels but the same SNR, or images with the same SNR but scanned faster (for example less averaging would be needed). It is likely that the second advantage yielding higher spatial resolution will be the principle clinical advantage of 7T.

The goal of this paper is to illustrate the potential advantages of 7T in clinical neuroimaging, by imaging a variety of neurological diseases at 7T and directly comparing them to lower field imaging (typically 3T) in the same patient.

Amytrophic lateral sclerosis	14
Dementia	1
Epilepsy	66
Multiple Sclerosis	18
Parkinsons disease	2
Traumatic brain injury	22
Tumors (brain)	6
Tumors (eye)	3
Vasculitis	2
Total	134

Sequences	$TR/TE_1/TE_2$ (ms)	FOV (mm^2)	Matrix	Slice thickness (mm)
Coronal FLAIR	8360/111	170	320 x 320	4
Axial FLAIR	8360/117	201	224 x 192	4
Axial 3D GRE	9.8/4.76	256	256 x 256	1
Coronal 3D GRE	11/4.92	230	224 x 256	1.25
Axial MPRAGE	1800/3.12	256	256 x 256	1
SWI	49/40	220	224 x 204	3

Table 1: 1.5T sequence parameters

Sequences	$TR/TE_1/TE_2$ (ms)	FOV (mm^2)	Matrix	Slice thickness (mm)
Coronal FLAIR	8100/115	180	240 x 192	3
Axial FLAIR	8640/128	180	256 x 204	3
Axial 3D GRE	4000/112	180	320 x 320	3
Coronal 3D GRE	10/4.6	256	256 x 256	1
Axial MPRAGE	1900/2.54	256	256 x 256	1
SWI	27/20	210	256 x 256	2.5

Table 2: 3T sequence parameters.

MRI technique

Currently the 7T system[1] is not FDA approved, and this study was approved by our institutional IRB for the strict purpose of comparing imaging features of neuropathology at 7T to imaging features obtained previously at lower field on an FDA approved clinical scanner. Exclusion criteria included implants not validated as safe at 7T, body weight less than 30 kg, inability to lay motionless while in MRI, claustrophobia, and a normal MRI at lower field.

The 7 tesla whole-body MRI system used at Cleveland Clinic is a Siemens MAGNETOM with an Agilent 830AS magnet. For all the studies presented here, a head-only CP transmit/32-channel phased-array receive coil (Nova Medical, Wilmington, MA, USA) was used. Sequences used in the following figures were: FLAIR, MP2RAGE, SWI, and GRE, as well as TSE T2 in the lower field scans. In order to focus on the qualitative features of the differences in imaging results, we list the complete scan protocols here and in individual figures highlight spatial resolution differences between the different field strength images. Although slight variations in clinical scan prescriptions exist across the scanner installations at Cleveland Clinic, the basic scan protocol for each at 1.5T and 3T are shown in Tables 1 and 2, respectively.

For 7T the scan protocols are:

Coronal and transverse 2D FLAIR TSE sequence
- TR/TE = 9000/124 ms
- FOV = 192 x 192 mm²
- slice number = 45
- slice thickness = 2 mm
- In-plane resolution = 0.75 x 0.75 mm²
- TI = 2600 ms
- matrix = 256 x 256
- GRAPPA 3
- bandwidth 244 Hz/pixel
- scan time = 3:02 min

Axial and/or sagittal T1-weighted MP2RAGE
- TR/TE = 6000/2.99 ms
- FOV = 240 x 240 mm²
- slice number = 192
- resolution = 0.75 mm³ isotropic voxel
- flip angle = 4° and 5°
- TI1/TI2 = 700/2600 ms
- Matrix = 320 x 320 6/8 partial Fourier in k_y and k_z
- GRAPPA 3
- bandwidth 240 Hz/pixel
- scan time = 9:48 min

T2*-weighted GRE
- TR/TE = 2290/17.8 ms
- FOV = 192 x 192 mm²
- slice number = 60
- slice thickness = 1.5 mm
- In-plane resolution = 0.38 x 0.38 mm²
- flip angle = 250
- matrix = 512 x 512
- GRAPPA 2
- bandwidth 40 Hz/pixel
- scan time =10:08 min

Transverse 3D SWI sequence
- TR/TE = 23/15 ms
- FOV = 220 x 220 mm²
- slice number = 144
- resolution = 0.49 x 0.49 x 0.8 mm³
- flip angle =20°

[1] MAGNETOM 7T is ongoing research. All data shown are acquired using a non-commercial system under institutional review board permission. MAGNETOM 7T is still under development and not commercially available yet. Its future availability cannot be ensured.

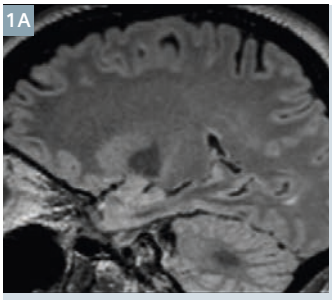

3T 5000/393/1800 [TR/TE/TI]

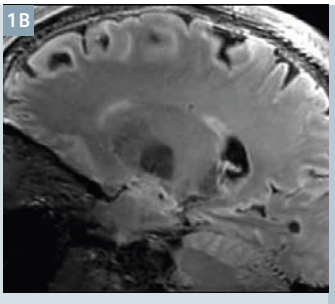

7T 7000/380/2100

1 Example of increased SNR in a FLAIR sequence from a 7T image **(1B)** compared to a 3T image **(1A)** in different patients. For comparison purposes, similar sequences were used that had the same voxel size (1 x 1 x 1 mm). In the flat region of anterior white matter, the SNR was 32.3 for 7T and 16.0 for 3T. While the increased SNR at 7T is apparent as a 'flatter' appearance of the white matter, this may not yield additional clinical benefit for most neurological disease, which would benefit more from using the increased SNR to enable smaller voxels and higher spatial resolution with the same SNR [5, 6].

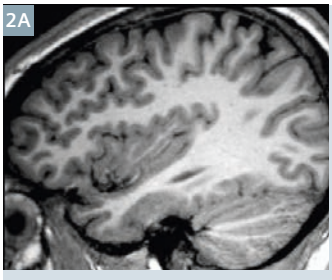

3T 1 x 1 x 1.2 mm
2300/2.98/900

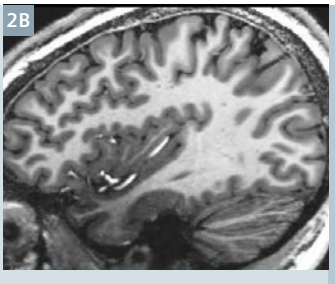

7T 0.75 x 0.75 x 0.75 mm
6000/2.99

2 Example of increased contrast-to-noise ratio (CNR) in a T1-weighted sequence, with 7T MP2RAGE **(2B)** and a 3T MPRAGE **(2A)**. The CNR of signal in white matter to gray matter is 18.3 (7T) and 9.9 (3T). This increased distinction between the gray-white interface is very important in the evaluation of a class of lesions causing epilepsy. In addition, any lesion embedded within white matter that follows gray matter signal characteristics will have increased conspicuity [7, 8].

3 Example of increased in-plane resolution, with 7T MP2RAGE **(3B)** and 3T MPRAGE **(3A)**. The in-plane voxel size is 0.75 x 0.75 mm (7T) and 1.0 x 1.0 mm (3T). Although the decrease in linear size is only 25%, this small change can noticeably improve image quality, as seen in the improved detail of the cerebellar folia. Also contributing to visual improvement at 7T is a thinner slice, being 0.75 mm compared with 1.2 mm for 3T, which provides less volume averaging and thereby sharper images [7-9].

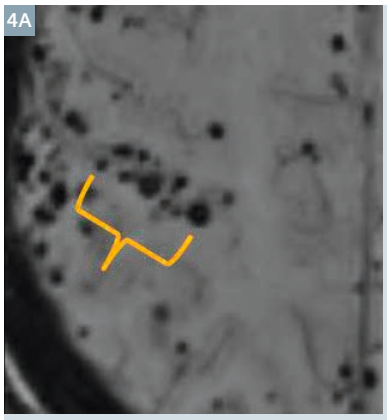

3T SWI 0.82 x 0.82 x 2.5 mm

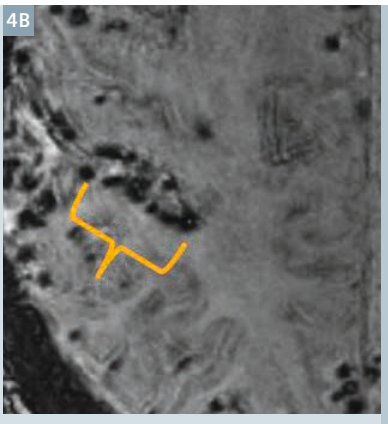

7T SWI 0.49 x 0.49 x 0.80 mm

4 Example of combination of increased spatial resolution and lesion conspicuity, enabling improved colocalization of small lesions on underlying anatomy. While this 64-year-old female already had a known diagnosis of cerebral amyloid angiopathy, manifest with innurable microhemorrhages (CMH) throughout the brain, the high spatial resolution of 7T revealed a strong colocalization of the CMH with the cortical ribbon. At lower field, this association could not be appriciated on the SWI sequence. Similar studies have shown the utility of 7T in the localization of microhemorrhages to the cortex in patients with cebebral amyloid angiopathy [10-12].

3T T2-TSE 0.55 x 0.55 x 4 mm thick

7T T2*-GRE 0.375 x 0.375 x 1.5 mm thick

5 Example of clinical utility in a multiple sclerosis patient. This 23-year-old female has a four-year history of progressive MS, whose diagnosis is not in question. This image examplifies a characteristic of MS well visualized with the high resolution of 7T, namely the central vein coursing through the middle of the MS plaque [14, 15]. The arrows point to the same plaque on a 3T T2-weighted sequence **(5A)**, and a 7T T2* GRE sequence **(5B)**. This imaging feature can be very useful in patients with lesser disease, where the diagnosis of MS is uncertain.

3T T2w 0.43 x 0.43 x 4 mm thick

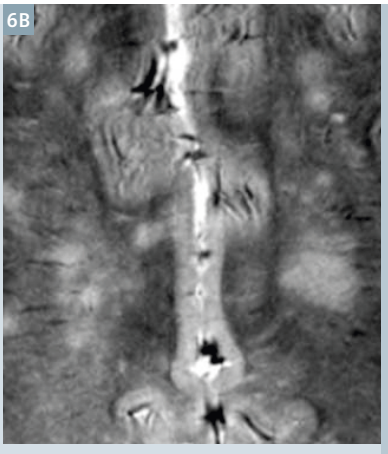

7T T2* GRE 0.375 x 0.375 x 1.5 mm thick

6 Counter-example to the previous patient of Figure 5 who had established MS. This 63-year-old female with cognitive issues has a heavy burden of white matter disease, and was referred to our mutiple sclerosis clinic for possible MS due to a 3T MRI. Images show a heavy burden of white matter disease, from a 3T T2-weighted sequence on the left **(6A)**, and a 7T T2* GRE sequence on the right **(6B)**. In distinction to the MS patient of Figure 5, no definitive central vein is seen at either field strength, and the diagnosis of MS was lowered, while the diagnosis of non-specific vasculopathy was raised [16]. A subseqent paratid biopsy revealed underlying Sjogren's disease, whose chronic small vessel disease likely caused the findings.

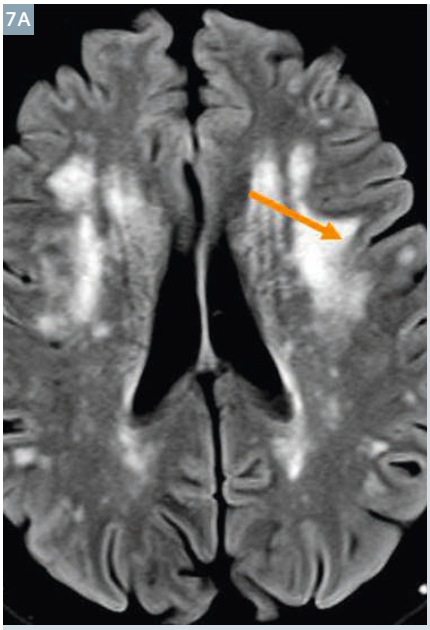

3T FLAIR 0.69 x 0.69 x 4 mm thick

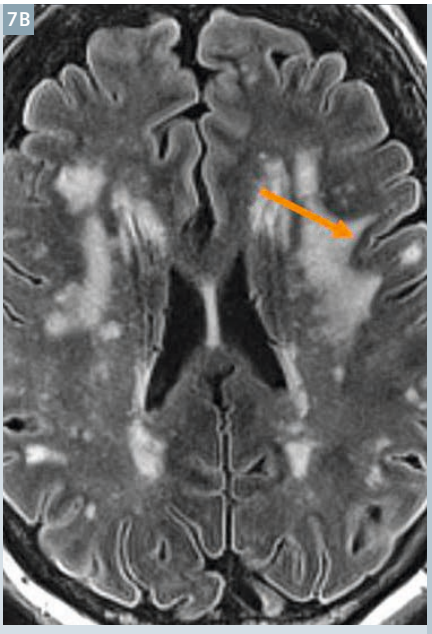

7T FLAIR 0.75 x 0.75 x 2 mm thick

7 Example of another discriminator of MS vs vasculopathy, using the same patient as in Figure 6. The subcortical U-fibers have a dual arterial blood supply (from both the adjacent capillary plexus occupying the gray matter ribbon, and from deep arterial penetrators coursing through the gray matter). This redundant supply of blood make this tissue more resiliant to ischemic injury, unlike deeper white matter. However, this tissue still remains as vulnerable to demyelinating disease as deeper white matter. Thus, careful delination of a preserved subcortical U-fibers can help discrimiate vasculopathy from demyelinating disease. In this case, the arrows point to a segment of subcortical U-fibers, which is better defined throughout (compare the segment just inferior to the arrows) with the high spatial resolution of 7T.

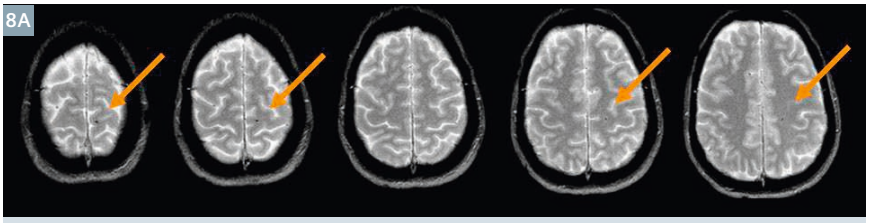

1.5T GRE 0.875 x 0.875 mm x 4 mm thick

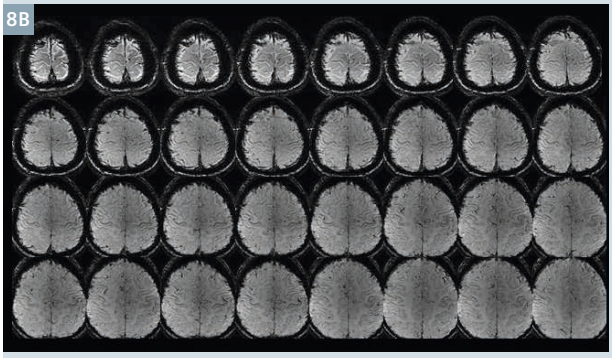

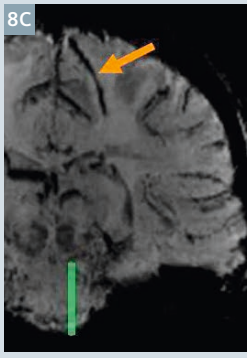

7T SWI 0.49 x 0.49 x 0.8 mm thick

8 Example of clinical value of small voxels and thin slices. A 43-year-old female presents six months after falling from a horse with headaches and presumed post-concussive syndrome. Several continuous slices from a 1.5T GRE sequence are shown in the top panel **(8A)**, with arrows pointing to small foci of susceptibility effect felt to be microhemorrhages. A 7T MRI was then obtained, bottom two panels **(8B, C)**. The lower panel shows an axial SWI sequence, whose 24 slices span the same axial distance as the 5 axial GRE slices at 1.5T. An advantage of the smaller voxels is that a high resolution MPR image was obtained in a coronal oblique direction **(8C)**, clearly revealing the dots of presumed microhemorrhage to be a linear morphology, and most likely a benign developmental venous anomaly, which is not related to traumatic brain injury (TBI). The patient has since been treated for chronic migraine headache, rather than post concussive syndrome. One similar study showed increased detection of developmental venous anomalies at 7T compared to 3T in patients with cavernous malformations [13].

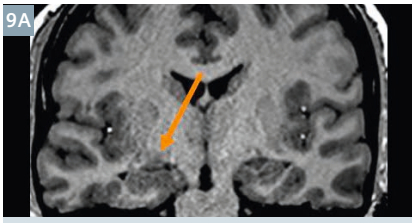

3T 0.41 x 0.41 x 1 mm

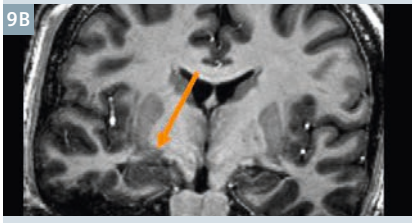

7T 0.75 x 0.75 x 0.75 mm

9 Example of a subtle heterotopia, never before appreciated at lower field MRI. The patient is a 30-year-old female, suffering from seizures since birth. A 7T T1 MP2RAGE **(9B)** revealed a previously unnoticed periventricular gray matter focus (arrow), lying adjacent to the right amygdala and hippocampus, which also appeared mildly enlarged. In addition, 7T revealed extensive periventricular heterotopias filling bilateral occipital horns (not shown). The patient recently underwent a right temporal lobectomy, and currently remains seizure free.

3T MPRAGE post gadolinium
0.45 x 0.45 x 2 mm thick

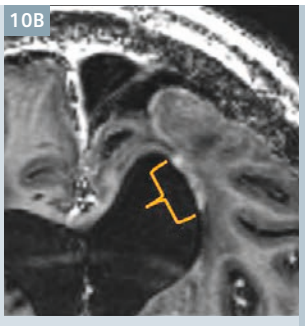

7T MP2RAGE post gadolinium
0.75 x 0.75 x 0.75 mm thick

10 Example of imaging recurrent tumor. This 65-year-old male has a known anaplastic oligodendroglioma, status post prior resection and radiation treatment. These post-gadolinium images (**10A**: 3T T1 MPRAGE; **10B**: 7T T1 MP2RAGE) show a thin segment of enhancement along the periventricular margin (shown by the bracket), indicative of tumor recurrence. While this 7T did not alter any clinical management, the high resolution and increased tissue contrast characteristics show better detail of the recurrence and adjacent tissue. This capability could potentially help patients because recurrence can be detected at a smaller level, earlier in the disease. Similarly, other studies have also shown increased tumor detection using different sequences at 7T compared to 3T [17-19].

3T SWI
0.43 x 0.43 mm x 2 mm thick

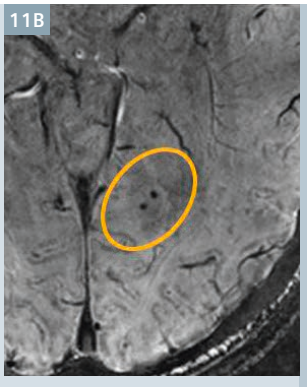

7T SWI
0.49 x 0.49 x 0.80 mm thick

11 Example of microhemorrhages not reported at lower field. This 54-year-old male experienced a motor vehicle accident 18 months earlier, and presents with persistant chronic headache. It is unclear if the headache is post-concussive syndrome, or a seperate headache syndrome. His 3T clinical MRI **(11A)** was reported as normal, however the 7T MRI **(11B)** showed several microhemorrhages with increased conspicuity. In retrospect, those microhemorrhages were visible with lower conspicuity at 3T. This example shows the practical importance of improved conspicuity of lesions, which is just as important as 7T revealing new lesions: if lesions with low conspicuity are present but not detected by the radiologist, they are effectively not present. On review of literature, one study has also shown 7T SWI improves identification of small hemorrhagic diffuse axonal injury compared to 3T [20].

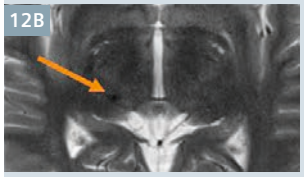

3T GRE 0.66 x 0.66 mm x 3 mm
and 3T T2-TSE
0.55 x 0.55 x 3 mm thick

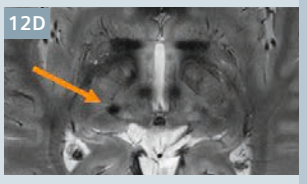

7T T2*-GRE
0.375 x 0375 x 2.00 mm thick

12 Another example of increased lesion conspicuity showing additional lesions. This 47-year-old male with a known cavernous malformation (shown on **12A, B** at 3T) had a 7T scan shown on **12C, D**. While the known large cavernous malformation in the posterior right insula shows increased detail at 7T, a second cavernous malformation not previously appreciated was seen in the right thalamus. In retrospect, this focus was present before but its marginal conspicuity was insufficient for a radiologist's detection. This lesion is now known and being followed. Prior earlier 7T studies using SWI have shown increased detection of a significant number of cavernous malformations and better definition of cavernous angioma angioarchitecture compared to lower fields [13, 21].

3T 0.28 x 0.28 x 3 mm

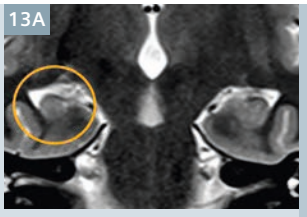

7T 0.375 x 0.375 x 1.50 mm

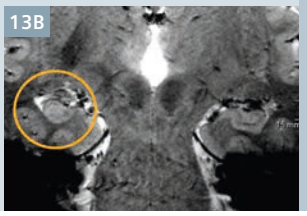

13 Example of high resolution confirming a diagnosis of mesial temporal sclerosis (MTS) in epilepsy. The patient is a 26-year-old male, who had a 3T MRI **(13A)** showing a rounded right hippocampal head (circled), slightly hyperintense, with indistinct internal architecture (compare those features with the patient's normal left hippocampus). 7T image **(13B)** provides superior definition of the rounded morphology and hyperintensity. This hippocampus was subsequently resected and the patient has now been seizure-free for over 2 years. While 7T did not change the diagnosis in this case, this example illustrates its potential to improve the diagnosis of MTS due to its superior resolution. Similarly, one study of 6 patients using 7T T2*-weighted sequence to evaluate hippocampal sclerosis showed greater anatomic detail than 1.5T [25].

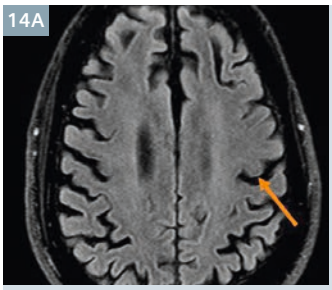

3T FLAIR
0.66 x 0.66 x 3 mm thick

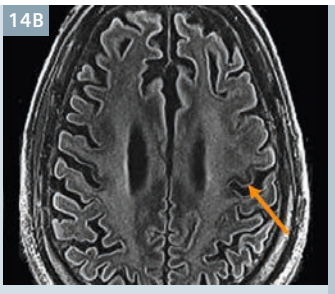

7T FLAIR
0.75 x 0.75 x 2 mm thick

14 Example of 7T applied to amytrophic lateral sclerosis (ALS), also known as Lou Gehrig's disease. The patient is a 68-year-old with ALS diagnosed 3 months earlier. **14A** is a 3T axial FLAIR, and **14B** a 7T axial FLAIR. The arrow points to the 'hand knob' of the motor strip in the left precentral gyrus. Note the gyriform decreased signal seen in the 7T, which is not well apparent at 3T. While this finding did not alter diagnosis or medical management, it has the potential to affect patients earlier in their disease when diagnosis may be ambiguous, as shown in other 7T studies [22-24].

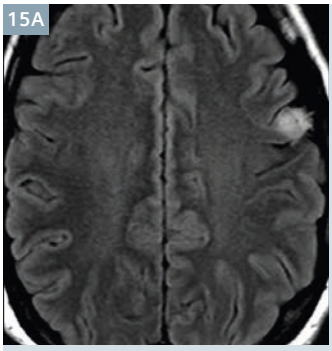

3T FLAIR
0.35 x 0.35 x 3 mm thick

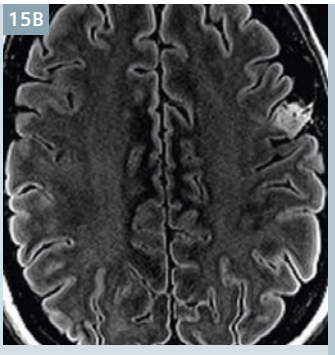

7T FLAIR
0.75 x 0.75 x 2.0 mm thick

15 Example left frontal lesion suspicious for a mass. This 31-year-old female presents with her first seizure in 25 years, after a history of childhood seizures. Images at 3T **(15A)** showed a left frontal lesion thought to be a low grade tumor, and was referred for possible resection. A 7T image **(15B)** provided sufficient detail to suggest the lesion is actually a post-traumatic lepto-meningeal cyst with subjacent scarring. The patient subsequently reported a prior history of head trauma at age 3 years. Surgery has been postponed and her seizures will be managed medically. This example shows increased lesion detail was able to alter the diagnosis of a tumor to a post-traumatic scar.

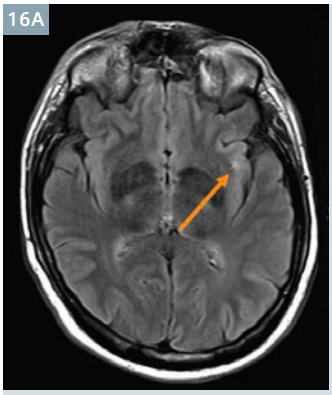

3T FLAIR
0.36 x 0.36 x 4 mm thick

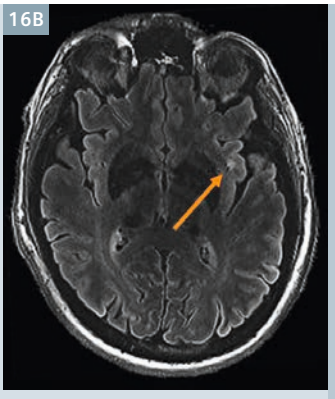

7T FLAIR
0.75 x 0.75 x 2.0 mm thick

16 Example of a lesion thought to be epilepstogenic, but determined to be benign with high resolution images. The patient is a 56-year-old male with epilepsy for 32 years, now medically refractory and being evaluated for surgery. A 3T FLAIR **(16A)** showed left subcortical gray-white indistinction of the insular cortex, suspicious for a focal cortical dysplasia. While this location was inconsistant with EEG findings, the patient was scheduled for an invasive neurosurgical evaluation to explore the lesion and other possible areas for seizure generation. A 7T FLAIR **(16B)** was obtained whose high resolution revealed the lesion to be a vascular abnormality causing adjacent scar that mimiced the appearance of a dysplasia. The patient's surgical plan was altered to not include the left insula.

3T FLAIR
0.35 x 0.35 x 3 mm thick

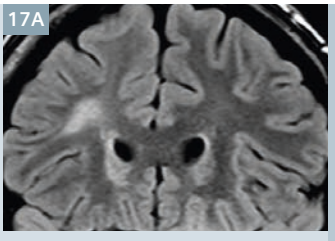

7T FLAIR
0.375 x 0.375 x 2 mm thick

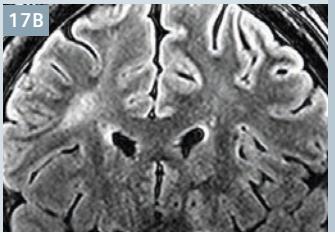

17 Example of ambiguous white matter lesion. The patient is a 24-year-old male with18 years of epilepsy. His 3T MRI image **(17A)** shows an unusual lesion in the right frontal lobe suggestive of a form of malformation of cortical development called a transmantle dysplasia. It was unclear if the lesion was related to his epilepsy because all his other tests pointed to posteriorly to this region. Higher detail due to smaller voxels from a 7T image **(17B)** verified that the lesion has no frank connection to the cortex, the adjacent cortex is normal with no gray-white indistinction, and the abnormality is most likely a vascular lesion. These features could be best appreciated by scrolling through the thin 7T sections. This suggestion was confirmed at 3T, and altered the patient's surgical plan to focus on other areas of the brain.

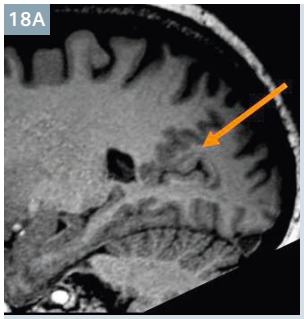

3T MPRAGE
0.41 x 0.41 x 1 mm

7T MP2RAGE
0.75 x 0.75 x 0.75 mm

18 Example of malformation of cortical development (MCD), not appreciated on imaging. The patient is a 37-year-old male with a 5-year history of epilepsy. His previous MRIs (typically 3T) only revealed a right thalamus cyst, which was known to be not epileptic. A 7T T1 MP2RAGE image **(18B)** showed an abnormal projection of gray matter signal extending into the white matter, compatible with a subcortical heterotopia (a form of MCD). In retrospect, guided by the 7T finding, subtle correlates could be found on 3T MRI **(18A)**. This identification of a subtle lesion started at 7T, and confirmed at 3T, altered the patient's management by making him a surgical candidate. This patient is currently undergoing intracranial EEG to confirm the epileptogenicity of the lesion.

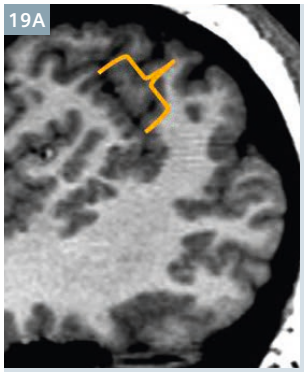

3T 0.46 x 0.46 x 0.94 mm

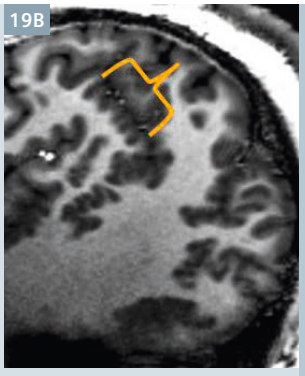

7T 0.75 x 0.75 x 0.75 mm

19 Example of improved conspicuity of Polymicrogyria (PMG). The patient is a 20-year-old male with a known congenital malformation of cortical development called PMG, manifest as abnormally small and tightly packed gyri (as an example, see cortex within interval of bracket). While the 3T sagittal MPGR image **(19A)** reveals the presence of PMG, the 7T MP2RAGE **(19B)** shows superior definition, due to combination of smaller voxels and increased CNR of gray to white matter. Occasionally regions of PMG are surgically removed, and accurate visualization of the extension is very important to clear surgical margins and potential cure. A study conducted by De Ciantis and colleagues also showed 7T provided additional details and greater involvement of cortical polymicrogyria compared to 3T, this was attributed to increased signal-to-noise and increased magnetic susceptibility [27].

3T T1-weighted
0.65 x 0.65 x 4 mm thick

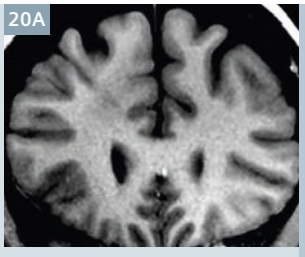

7T MP2RAGE
0.75 x 0.75 x 0.75 mm

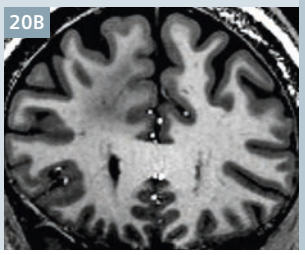

20 Example of low-grade brain tumor. The patient is a 50-year-old female, with a 15-year history of biopsy proven low grade astrocytoma, which had been grossly stable during that time. In addition, she had a 40-year history of epilepsy, well controlled until recently, and was now under consideration for surgery. A 3T coronal T1-weighted image **(20A)** shows subtle signal abnormality in the right frontal lobe white matter. The corresponding 7T image **(20B)** redemonstrates this finding with greater conspicuity. This detail improved visualization of the tumor's margins, which were more extensive than originally thought, and guided the decision to continue medical management rather than undergo a larger brain surgery. Another 7T study used a different approach and different set of sequences to evaluate 15 patients with astrocytomas (WHO grades II-IV) – greater susceptibility was used to detect tumor margins by observation of tumor vascularity which was only present at lower grade as diffusely infiltrating astrocytoma [18].

Discussion

One weakness of this method of using a gallery of side-by-side image comparisons of 7T to lower field to assess any clinical utility is that it only assesses the two-dimensional image. Our experience is that when actively viewing images on a DICOM viewer, with the ability to scroll up and down through lesions, and actively window, markedly increased lesion conspicuity, as opposed to simply viewing one static image. Thus, any conspicuity of images shown in this paper should be qualitatively considered a lower limit.

Another weakness is that the 7T protocols used in this study are not clincally optimized in terms of scanning time, as are the refined protocols on clinical MRIs at lower field. Imaging slots on the 7T do not face the same adminstrative pressures for patient throughput as clinical magnets, and are currently more liberal with scan times. Note this increased time is not unexpected at this early stage in the evolution of clinical sequence and protocol development at 7T. Thus, in the future, a more valid clinical comparison might involve using common sequences and protocols at 7T and lower field that require the same scan time.

Another limitation of the clinical utility of 7T is the increased B_1 inhomogeneities compared with lower field strength scanning. This presents a problem for interpretation of

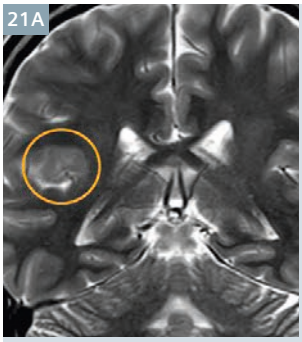

3T 0.28 x 0.28 x 3 mm

7T 0.375 x 0.375 x 2 mm

21 Example of subtle right peri-insular malformation of cortical development. This patient is a 26-year-old male who had intractable epilepsy for 19 years. EEG showed that seizures were originating from the left frontotemporal area. Coronal 3T T2-weighted image **(21A)** showed a suspicious lesion in the right posterior insular/parietal operculum region. 7T coronal GRE image **(21B)** delineated the lesion with much better conspicuity. The patient underwent surgery with complete resection of the subtle right peri-insular lesion and is now seizure free. Pathology confirmed a severe focal cortical dysplasia. A similar 7T study of patients with intractable focal epilepsy and unrevealing lesions, showed 26% improved detection of epileptogenic lesions not seen on 1.5T or 3T [26].

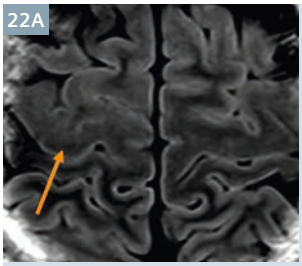

3T 0.82 x 0.82 x 4 mm

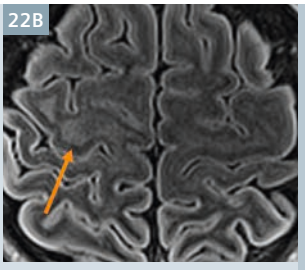

7T 0.75 x 0.75 x 2 mm

22 Example of subtle cortical dysplasia in epilepsy. The patient is an 18-year-old female with refractory focal epilepsy, with multiple prior 3T MRIs all read as normal. A 7T axial FLAIR image **(22B)** showed abnormally increased and asymmetric subcortical hyperintensity (arrow), which was also hypointense with indistinct gray-white margins on T1 MPRAGE sequence (not shown). In retrospect, a subtle abnormality could be seen at 3T **(22A)**, but with much less conspicuity and only on the exact same slice. The lesion was resected, with pathology confirming a focal cortical dysplasia. The patient remains seizure free.

whole-brain images, particularly in the lower parts of the temporal lobe, an important region for consideration of surgical intervention in epilepsy. Head coils incorporating multiple parallel transmission coil elements show considerable promise to improve the whole-brain B_1 homogeneity [28].

This paper presents a gallery of images of various neurological diseases, portrayed as a side-by-side comparison of 7T to lower field, each obtained in the same patient. This wide ranging comparison is made possible by an IRB permitting imaging of clinical patients at 7T for the expressed comparison of those imaging findings to those already obtained at lower field. Often this prompted a reappraisal of the earlier lower field findings and occassionally affected patient management.

The visualization of a lesion at 7T that was frankly not visible at lower field was infrequent, and typically the lesion was visible on the lower field image but less conspicuous. Sometimes this decerased conspicuity meant the lesion was not noticed at lower field by the radiolgoist. Therefore, in a busy clinical practice, there could be value for 7T imaging that increases lesion conspicuity that enables a radiolgist's detection, and this improvement is just as important as any de novo appearance of new lesions at 7T.

This series of cases includes clinical vignettes decribing how 7T findings influenced clinical management. While a few cases showed new, or de facto new lesions (such as Figure 8 microhemorrhages in TBI), the majority simply showed lesions visible at lower field, but with greater conspicuity. This increase is mainly due to smaller voxels providing higher spatial resolution, perhaps accentuated by intrinsically increased contrast-to-noise ratio of different tissue types. While the linear decrease in voxel size at 7T may seem modest (around 25%), this small increase nonetheless greatly aids lesion discrimiation to the radiologist's eye.

It is difficult to exactly predict the future clinical niche of 7T in neurological imaging. Some guidance of the extension from 3T to 7T may come from our prior experience from the extension from 1.5T to 3T [29-33]. Today 3T clincial image quality is superb but the initial MRIs suffered from inhomogenities. There were early concerns about differences of tissue contrast, gadolinium contrast, and poor coils [34, 35]. Today with over a decade of continued development and experience, 3T MRI addressed these issues and is now a mainstay of clinical imaging when high resolution and quality are required, for example in epilepsy. While the costs for 7T will be considerably more than 3T, there may likely evolve many clinical applications where 7T imaging will be specifically sought, especially after an analogous decade of continued developement and improvement [36].

Lastly, the role of 7T could borrow from an analogy in the technology of television, and its recent adoption of high-definition television (HDTV): 7T could viewed as 'high definition MRI'. In this analogy, whereas a television viewer can generally enjoy a program in both low-definition and high-definition TV, occassionally the extra detail makes a difference, for example when viewing the scores displayed during a sports broadcast. Similarly with MRI, both low-field and 7T can show important radiological features, but occassionally the extra resolution makes an important clinical difference.

Conclusion

The greatest clinical utility of 7T may be its improved spatial resolution, which can aid in the clinical diagnosis of pathologies that contain fine detail. A second utility may be its increased sensitivity to susceptibility effects. Finally, while 7T infrequently showed new lesions not frankly visible at lower field, it shows lesions better, and this can provide clinical significance.

References

1 Hua J, Qin Q, van Zijl PCM, et al. Whole-brain three-dimensional T2-weighted BOLD functional magnetic resonance imaging at 7 Tesla. Magn Reson Med 2014;72:1530–40.
2 Harmer J, Sanchez-Panchuelo RM, Bowtell R, et al. Spatial location and strength of BOLD activation in high-spatial-resolution fMRI of the motor cortex: a comparison of spin echo and gradient echo fMRI at 7 T. NMR Biomed 2012;25:717–25.
3 van der Zwaag W, Francis S, Head K, et al. fMRI at 1.5, 3 and 7 T: characterising BOLD signal changes. Neuroimage 2009;47:1425–34.
4 Olman CA, Yacoub E. High-field FMRI for human applications: an overview of spatial resolution and signal specificity. Open Neuroimag J 2011;5:74–89.
5 Vaughan JT, Garwood M, Collins CM, et al. 7T vs. 4T: RF power, homogeneity, and signal-to-noise comparison in head images. Magn Reson Med 2001;46:24–30.
6 Pohmann R, Speck O, Scheffler K. Signal-to-noise ratio and MR tissue parameters in human brain imaging at 3, 7, and 9.4 tesla using current receive coil arrays. Magn Reson Med 2016;75:801–9.
7 Shin W, Shin T, Oh S-H, et al. CNR improvement of MP2RAGE from slice encoding directional acceleration. Magn Reson Imaging 2016;34:779–84.
8 Seiger R, Hahn A, Hummer A, et al. Voxel-based morphometry at ultra-high fields. a comparison of 7T and 3T MRI data. Neuroimage 2015;113:207–16.
9 Fujimoto K, Polimeni JR, van der Kouwe AJW, et al. Quantitative comparison of cortical surface reconstructions from MP2RAGE and multi-echo MPRAGE data at 3 and 7 T. Neuroimage 2014;90:60–73.
10 Ni J, Auriel E, Martinez-Ramirez S, et al. Cortical localization of microbleeds in cerebral amyloid angiopathy: an ultra high-field 7T MRI study. J Alzheimers Dis 2015;43:1325–30.
11 van Veluw SJ, Biessels GJ, Klijn CJM, et al. Heterogeneous histopathology of cortical microbleeds in cerebral amyloid angiopathy. Neurology 2016;86:867–71.
12 De Reuck J, Deramecourt V, Cordonnier C, et al. Superficial siderosis of the central nervous system: a post-mortem 7.0-tesla magnetic resonance imaging study with neuropathological correlates. Cerebrovasc Dis 2013;36:412–7.
13 Frischer JM, Göd S, Gruber A, et al. Susceptibility-weighted imaging at 7 T: Improved diagnosis of cerebral cavernous malformations and associated developmental venous anomalies. NeuroImage Clin 2012;1:116–20.
14 Tallantyre EC, Morgan PS, Dixon JE, et al. 3 Tesla and 7 Tesla MRI of multiple sclerosis cortical lesions. J Magn Reson Imaging 2010;32:971–7.
15 Ge Y, Zohrabian VM, Grossman RI. Seven-Tesla magnetic resonance imaging: new vision of microvascular abnormalities in multiple sclerosis. Arch Neurol 2008;65:812–6.
16 Kilsdonk ID, Wattjes MP, Lopez-Soriano A, et al. Improved differentiation between MS and vascular brain lesions using FLAIR* at 7 Tesla. Eur Radiol 2014;24:841–9.
17 Noebauer-Huhmann I-M, Szomolanyi P, Kronnerwetter C, et al. Brain tumours at 7T MRI compared to 3T--contrast effect after half and full standard contrast agent dose: initial results. Eur Radiol 2015;25:106–12.
18 Moenninghoff C, Maderwald S, Theysohn JM, et al. Imaging of adult astrocytic brain tumours with 7 T MRI: preliminary results. Eur Radiol 2010;20:704–13.
19 Paek SL, Chung YS, Paek SH, et al. Early experience of pre- and post-contrast 7.0T MRI in brain tumors. J Korean Med Sci 2013;28:1362–72.
20 Moenninghoff C, Kraff O, Maderwald S, et al. Diffuse axonal injury at ultra-high field MRI. PLoS One 2015;10:e0122329.
21 Dammann P, Wrede K, Zhu Y, et al. Correlation of the venous angioarchitecture of multiple cerebral cavernous malformations with familial or sporadic disease: a susceptibility-weighted imaging study with 7-Tesla MRI. J Neurosurg http://doi.org/10.3171/2016.2.JNS152322.
22 Cosottini M, Donatelli G, Costagli M, et al. High-Resolution 7T MR Imaging of the Motor Cortex in Amyotrophic Lateral Sclerosis. AJNR Am J Neuroradiol 2016;37:455–61.
23 Versluis MJ, van der Grond J, van Buchem MA, et al. High-field imaging of neurodegenerative diseases. Neuroimaging Clin N Am 2012;22:159–71, ix.
24 Kwan JY, Jeong SY, Van Gelderen P, et al. Iron accumulation in deep cortical layers accounts for MRI signal abnormalities in ALS: correlating 7 tesla MRI and pathology. PLoS One 2012;7:e35241.
25 Breyer T, Wanke I, Maderwald S, et al. Imaging of patients with hippocampal sclerosis at 7 Tesla: initial results. Acad Radiol 2010;17:421–6.
26 De Ciantis A, Barba C, Tassi L, et al. 7T MRI in focal epilepsy with unrevealing conventional field strength imaging. Epilepsia 2016;57:445–54.
27 De Ciantis A, Barkovich AJ, Cosottini M, et al. Ultra-high-field MR imaging in polymicrogyria and epilepsy. AJNR Am J Neuroradiol 2015;36:309–16.
28 Zhu, Y: Parallel excitation with an array of transmit coils. Magnetic resonance in medicine, 51, 775-84, (2004).
29 Lin W, An H, Chen Y, et al. Practical consideration for 3T imaging. Magn Reson Imaging Clin N Am 2003;11:615–39, vi.
30 Frayne R, Goodyear BG, Dickhoff P, et al. Magnetic resonance imaging at 3.0 Tesla: challenges and advantages in clinical neurological imaging. Invest Radiol 2003;38:385–402.
31 Shapiro MD, Magee T, Williams D, et al. The time for 3T clinical imaging is now. AJNR Am J Neuroradiol 2004;25:1628–9; author reply 1629.
32 Pattany PM. 3T MR imaging: the pros and cons. AJNR Am J Neuroradiol 2004;25:1455–6.
33 Schmitz BL, Aschoff AJ, Hoffmann MHK, et al. Advantages and pitfalls in 3T MR brain imaging: a pictorial review. AJNR Am J Neuroradiol 2005;26:2229–37.
34 Runge VM, Case RS, Sonnier HL. Advances in clinical 3-tesla neuroimaging. Invest Radiol 2006;41:63–7.
35 Alvarez-Linera J. 3T MRI: advances in brain imaging. Eur J Radiol 2008;67:415–26.
36 Schmitt F, Grosu D, Mohr C, et al. [3 Tesla MRI: successful results with higher field strengths]. Radiologe 2004;44:31–47.

Contact

Stephen Jones, M.D., Ph.D.
Diagnostic Radiology
Cleveland Clinic Main Campus
Mail Code U15
9500 Euclid Avenue
Cleveland, OH 44195
USA
Phone: +1 216.444.4454
joness19@ccf.org